NMR and SANS Studies of Aggregation and Microemulsion Formation by Phosphorus Fluorosurfactants in Liquid and Supercritical Carbon Dioxide

Bin Xu,[†] Gary W. Lynn,[‡] Ji Guo,[†] Yuri B. Melnichenko,[‡] George D. Wignall,[‡] James B. McClain,[§] Joseph M. DeSimone,[†,⊥] and Charles S. Johnson, Jr.*,[†]

Department of Chemistry, University of North Carolina, Chapel Hill, North Carolina 27599; Center for Neutron Scattering, Oak Ridge National Laboratory,[#] Oak Ridge, Tennessee 37831-6393; Micell Technologies, Inc., 7516 Precision Drive, Raleigh, North Carolina 27617; and Department of Chemical Engineering, North Carolina State University, Raleigh, North Carolina 27695

Received: January 27, 2005

^{1}H NMR relaxation and diffusion studies were performed on water-in-CO_2 (W/C) microemulsion systems formed with phosphorus fluorosurfactants of bis[2-(F-hexyl)ethyl] phosphate salts (DiF_8), having different counterions (Na^+, NH_4^+, $N(CH_3)_4^+$) by means of high-pressure in situ NMR. Water has a low solubility in CO_2 and is mainly solubilized by the microemulsion droplets formed with surfactants added to CO_2 and water mixtures. There is rapid exchange of water between the bulk CO_2 and the microemulsion droplets; however, NMR relaxation measurements show that the entrapped water has restricted motion, and there is little "free" water in the core. Counterions entrapped by the droplets are mostly associated with the surfactant headgroups: diffusion measurements show that counterions and the surfactant molecules move together with a diffusion coefficient that is associated with the droplet. The outer shell of the microemulsion droplets consists of the surfactant tails with some associated CO_2. For W/C microemulsions formed with the phosphate-based surfactant having the ammonia counterion (A-DiF_8), the ^{1}H NMR signal for NH_4^+ shows a much larger diffusion coefficient than that of the surfactant tails. This apparent paradox is explained on the basis of proton exchange between water and the ammonium ion. The observed dependence of the relaxation time (T_2) on W_0 (mole ratio of water to surfactant in the droplets) for water and NH_4^+ can also be explained by this exchange model. The average hydrodynamic radius of A−DiF_8 microemulsion droplets estimated from NMR diffusion measurements (25 °C, 206 bar, $W_0 = 5$) was $R_h = 2.0$ nm. Assuming the theoretical ratio of $R_g/R_h = 0.775$ for a solid sphere, where R_g is the radius of gyration, the equivalent hydrodynamic radius from SANS is $R_h = 1.87$ nm. The radii measured by the two techniques are in reasonable agreement, as the two techniques are weighted to measure somewhat different parts of the micelle structure.

Introduction

Liquid/supercritical carbon dioxide (CO_2) is an ideal solvent candidate for material synthesis and processing. While it is a good solvent for many different small molecules such as methanol and *N*-methylpyrrolidinone, the low solubilities of many polar (salts, water, proteins) molecules restrict applications of CO_2 in many areas. To alleviate this problem, surfactants have been developed that self-assemble to form water-in-CO_2 (W/C) microemulsions. With the assistance of grafted copolymers[1] or specially designed surfactants,[2−4] stable and transparent microemulsion systems have been achieved that can disperse water and other solutes.

Most of the surfactants that form W/C microemulsions are anionic and have fluorocarbon tails that are easily solvated by CO_2[5,6] such as the fluorinated analogues of AOT (Aerosol-OT),[7] the ammonium carboxylate perfluoropolyether (PFPE-$COO^-NH_4^+$),[2] and the phosphorus fluorosurfactants.[3,8] The W/C microemulsion systems formed with $PFPECOO^-NH_4^+$ have been intensively studied by means of FT-IR, fluorescence, UV−vis absorption, electron paramagnetic resonance spectroscopy (EPR), small-angle X-ray scattering (SAXS), small-angle neutron scattering (SANS), and high-pressure NMR technology.[2,9−15] It has been found that the microemulsion droplets aggregate and form networks with water channels at high surfactant concentrations and lower pressures.[15] Unfortunately, $PFPECOO^-NH_4^+$ samples vary from batch to batch since it is a polymer mixture, and this feature complicates data analysis and quantitative understanding of the system.

In this work we focus attention on phosphorus fluorosurfactants of bis[2-(F-hexyl)ethyl] phosphate salts (DiF_8) synthesized in-house with different counterions including Na^+, NH_4^+, and $N(CH_3)_4^+$. These materials have precisely known compositions, and their solubility in CO_2 depends on the particular counterions. We have determined the conditions under which microemulsions form, the structure of the microemulsion droplets, their capacity for solvating water, the mobility of entrapped water, and droplet diffusion coefficients as a function of density.

As illustrated in Scheme 1 (confirmed by SANS measurements),[16] water molecules are entrapped inside the microemulsion droplets and are also present at low concentrations in the CO_2 continuous phase. As in the $PFPECOO^-NH_4^+$ case, there is rapid exchange of water molecules between the bulk CO_2 phase and the droplets. In contrast to this behavior, counterions

[†] University of North Carolin.
[‡] Oak Ridge National Laboratory.
[§] Micell Technologies, Inc.
[⊥] North Carolina State University.
[#] Managed by UT-Battelle, LLC under contract DE-AC05-00OR22725 with the U.S. Department of Energy.
* To whom correspondence should be addressed: Fax (919) 843-6041; Ph (919) 966-5229; e-mail charles_johnson@unc.edu.

10.1021/jp0580322 CCC: $30.25
Published on Web 04/21/2005

SCHEME 1. W/C Micromulsion Structure

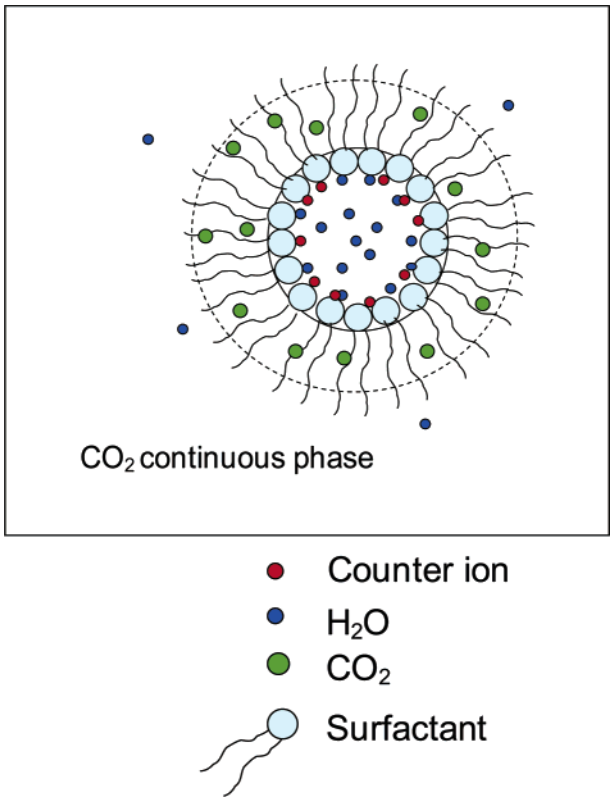

are entirely entrapped inside the droplets and are mostly associated with the headgroups. A shell region composed of surfactant tails and some associated CO_2 exists between the headgroups in the droplets and the CO_2 continuous phase. The diffusion coefficient of the droplets was obtained by measuring either the diffusion coefficient of the surfactant tails or the entrapped counterions. In the case of the microemulsions formed with A−DiF_8 (NH_4^+−DiF_8) in the presence of water, the effective diffusion coefficient of NH_4^+ as determined by PFG-NMR is larger than that of the surfactant tails. A simple two-site exchange model for the protons is proposed to explain this diffusion phenomenon and the observed dependence of relaxation times (T_2) for water and NH_4^+ on W_0 (mole ratio of water to surfactant). This is an interesting situation where the proton transfer between water and NH_4^+ is slow on the chemical shift scale where separate signals are observed for water and NH_4^+ but fast in the NMR diffusion experiment where the time scale is determined by the diffusion time selected, i.e., the time between gradient pulses.

No evidence was found for droplet aggregation and network formation, but that may reflect the lower concentration ranges accessible to the DiF_8 systems. Complementary SANS measurements are sensitive to the water droplet (core) dimensions and provided an estimate of their size and the variation with pressure and temperature. NMR diffusion measurements provided a hydrodynamic radius that was similar to the SANS dimensions, and we discuss possible reasons for the slight (~7%) discrepancies.

Experimental Section

Materials. Carbon dioxide (SFE/SFC grade, >99.9999%, with dip tube, no helium headspace) was supplied by Air Products (Allentown, PA) and was used as received. Distilled water was used throughout the measurements. The phosphate fluorosurfacants, bis[2-(F-hexyl)ethyl] phosphate salts with

SCHEME 2. DiF_8 Series Surfactants

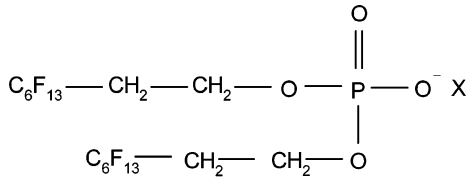

X: $-Na^+$	$Na\text{-}DiF_8$	M_w: 812 g/mol
$-NH_4^+$	$A\text{-}DiF_8$	M_w: 807g/mol
$-N(CH_3)_4^+$	$TMA\text{-}DiF_8$	M_w: 880g/mol

different counterions (DiF_8 series surfactants, as shown in Scheme 2), were synthesized following the method developed by Keiper et al.[3,4] Sample purity was confirmed by ^1H, ^{19}F, and ^{31}P NMR spectra.

High-Pressure Sample Delivery and Mixing Setup. The high-pressure setup was the same as previously described,[15] except for the high-pressure NMR cell. An NMR cell machined from PEEK replaced our previously used capillary cell. Details about the PEEK cell have been presented elsewhere.[17]

NMR Facilities. NMR measurements were performed with a Bruker Avance 500 spectrometer operating at 500.13 MHz for proton (^1H) observation. The detection region of a 5 mm Nalorac diffusion probe was calibrated to 25.0 ± 0.1 °C with a thermocouple. One-dimensional NMR spectra were obtained with a single 20° pulse and a 5 s relaxation recovery delay. For ^1H spectra 16K data points were typically acquired for a 14 ppm (700 Hz) spectral width, and 64 transients were accumulated to achieve satisfactory signal-to-noise ratios (S/N). The resonances were integrated, after automatic polynomial baseline correction, with the xwinnmr program (Bruker, version 2.6). The bipolar pulse pair longitudinal eddy current delay (BPP-LED) sequence[18] was used for the diffusion measurements (relaxation delay of 2 s, gradient pulse width $\delta = 2$ ms, separation in BPP $\tau = 1$ ms, diffusion time typically $\Delta = 6.5$ ms, longitudinal eddy current delay $T_e = 200$ μs, 64 transients accumulated after 32 steady-state dummy scans). Rectangular gradient pulses were used, and the diffusion coefficients were obtained by fitting acquired data points with the following equation[18]

$$S(q) = S(0)\exp(-Dq^2\Delta_r) \quad (1)$$

where $S(q)$ is the signal intensity, D is the tracer diffusion coefficient, $q = \gamma g\delta$, γ is the gyromagnetic ratio, g is the gradient amplitude (0−1.03 T/m), and $\Delta_r = \Delta - \delta/2 - \tau/2$ with the time intervals defined above.

The longitudinal relaxation times (T_1) were measured with the conventional inversion recovery sequence. The apparent transverse relaxation times (T_2) for H_2O and NH_4^+ protons were estimated from line widths in the one-dimensional spectra after a correction for field inhomogeneity and were confirmed by the Hahn spin echo experiment.

Small-Angle Neutron Scattering (SANS) Facilities. Measurements were carried out on the NG3 30m SANS instrument at the National Institute of Standards and Technology Center for High-Resolution Neutron Scattering. A sample−detector distance of 8 m and incident wavelength of $\lambda = 6$ Å were used to give an overall range of momentum transfer $0.0050 < Q = 4\pi\lambda^{-1}\sin\theta < 0.070$ Å^{-1}, where 2θ is the angle of scatter. The experiments were conducted in a cell that has been used extensively for previous neutron scattering experiments,[3,4] with 23.1 mm path length (5.6 cm^3 volume), and because of the high penetrating power of neutrons, the beam passed through two

~1 cm thick sapphire windows with virtually no parasitic scattering or attenuation (cell transmission ~93%). All data sets were corrected for instrumental backgrounds and normalized to an absolute scale by measuring the direct beam flux. To correct for the background scattering from the gaseous medium, we first measured CO_2 at two different pressures [149 bar (2154 psi) and 369.3 bar (5373 psi)]. These backgrounds differed by typically ~0.01 cm^{-1} and were then subtracted from the "sample" data with the same CO_2 pressure.

Results and Discussion

In previous studies of $PFPECOO^-NH_4^+$ in a capillary sample cell, it was found that the proton T_1 values depended on the time delay between sample recirculation and data acquisition. It was suggested that shear forces on the microemulsions during recirculation through the multiple bends of the folded capillary bunch disrupted the microemulsion structure, perhaps homogenizing the mixture, and that a new equilibrium was only slowly attained.[15] In the present study which used a much larger sample cell made from PEEK, the dependence of relaxation times on the delay time was not significant, probably indicating that shear forces in the PEEK cell (i.d. = 1.4 mm) were reduced and have less effect on the microemulsion structure. Of course, it is possible that the DiF_8 microemulsions equilibrate more rapidly, especially at the lower concentrations investigated. The PEEK cell was not used in studies of $PFPECOO^-NH_4^+$ nor was the capillary cell used to analyze the DiF_8 surfactant system used here. In the systems formed with $Na-DiF_8$, the measured T_1, T_2, and D values remained relatively constant as the recirculation time was increased from 10 to 40 min. When the waiting time between each recirculation and measurement was changed from 1 to 8 h, these values remained unchanged. With $A-DiF_8$ systems the recirculation time did not affect the measured T_1, T_2, and D values for protons on the surfactant tails, but the waiting time did have a significant effect on T_1 and T_2 values for NH_4^+ and H_2O, even though their D values were unaffected. In the later discussion the related values for $A-DiF_8$ systems were all measured after equilibrium was reached.

Diffusion Behavior. The use of PEEK cells with larger i.d.'s increases the probability of interference from mass convection during diffusion measurements. In our previous work[17] on diffusion of water dissolved in liquid CO_2, we found that the interference is significant when the temperature is much higher than room temperature (25 °C), e.g., at 35 °C. For measurements at 25 °C, this effect is small and is responsible for errors of less than 5% in diffusion coefficients for water dissolved in CO_2. Fortunately, in W/C microemulsion systems formed with $Na-DiF_8$, where the viscosity is larger, this effect is even smaller, around 3%. Since 3% is an acceptable error, we have chosen the standard BPPLED sequence rather than the convection suppression sequence[19] that requires a much longer time for data acquisition.

We investigated the effects of pressure and W_0 on diffusion coefficients (D) of water and surfactants in the W/C microemulsion systems formed with $Na-DiF_8$ and $TMA-DiF_8$ at 25 °C. Here W_0 is the mole ratio of water to surfactant (in microemulsion droplets**)** properly corrected for the solubility of water in the CO_2 continuous phase.[20]

In Figure 1A the diffusion coefficients of water (D_{water}) and surfactant (D_{surf}) in the W/C microemulsion system formed with $Na-DiF_8$ at varied pressures are presented with the surfactant concentration of 7 wt % and $W_0 \approx 9$. In the $PFPECOO^-NH_4^+$ microemulsion system a sharp increase in D_{water} was found in the low CO_2 density range. This phenomenon was attributed to the formation of "water channels" through which water could diffuse as in bulk water.[15] In contrast to this behavior, we find no significant increase in D_{water} for the $Na-DiF_8$ system in the low CO_2 density region. We conclude that under our experimental conditions droplet aggregation, channel formation, and percolation do not occur.

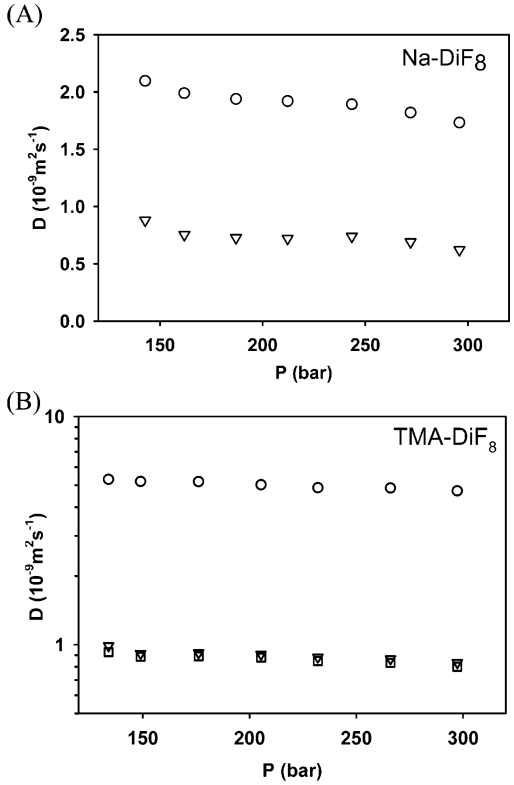

Figure 1. (A) Diffusion coefficients of water (○) and surfactant tails (DiF_8,▽) at various pressures for the W/C microemulsions formed with $Na-DiF_8$ (25 °C, $Na-DiF_8$ 7 wt %, W_0 around 9). (B) Diffusion coefficients of components in W/C microemulsions formed with $TMA-DiF_8$ at 25 °C, $TMA-DiF_8$ 2.5 wt %, W_0 around 4.5: water (○), surfactant tails (DiF_8,▽), and counterions (TMA, □).

The diffusion coefficient of microemulsion droplets (D_{ME}) is represented by D_{surf}, and we see that D_{water} is much larger than D_{ME}. As discussed previously,[15] water molecules transfer rapidly between the CO_2 continuous phase and the interior of the microemulsion droplets, and the measured D_{water} is the weighted average of the diffusion coefficients of the two sites for water as shown in eq 2:

$$D_{water} = f_A D_{water/CO_2} + (1 - f_A) D_{ME} \quad (2)$$

where f_A is the fraction of water dissolved in the CO_2 continuous phase. D_{water/CO_2} at various pressures has been reported,[17] and $D_{ME} = D_{surf}$ as noted above. The result is that D_{water} is much larger than D_{ME}. The value of f_A computed with eq 2 was found to agree with that computed with reference solubility data,[20] thus confirming the consistency of this treatment.

With the assumption that the W/C microemulsion droplets behave as hard spheres, the hydrodynamic radius (R_h) of the droplets was estimated to be between 2 and 3 nm on the basis of the Stokes−Einstein equation $R_h = k_B T/(b\pi\eta D)$, where k_B is the Boltzmann constant, T is temperature, D is the tracer diffusion coefficient, η is the viscosity of the solvent, and $b = 6$ for "stick" boundary conditions. The R_h value is larger than the fully stretched length of the surfactant excluding counterion (2.03 nm) estimated from geometry,[21] confirming the existence

of microemulsion structures. In Figure 1B the diffusion coefficients of water (D_{water}), counterion (D_{TMA}), and surfactant (D_{surf}) at various pressures in the TMA−DiF_8 system are shown for a surfactant concentration of 2.5 wt % and $W_0 \simeq 4.5$. As with the Na−DiF_8 system, no significant increase of D_{water} appeared in the low CO_2 density range, again indicating no evidence of percolation behavior for the TMA−DiF_8 system under these conditions. D_{TMA} is approximately equal to D_{surf}, indicating that the counterions are entrapped and diffusing with the surfactant tails, i.e., $D_{ME} \cong D_{surf} \cong D_{TMA}$. Also, $D_{water} > D_{ME}$ as expected from the exchange model discussed above.

The effects of W_0 on diffusion coefficients in the Na−DiF_8 and TMA−DiF_8 systems are shown in Figure 2A,B. In both figures, diffusion coefficients of surfactant tails (and also the counterions in the TMA−DiF_8 system) decrease slightly as the W_0 values are increased. We attribute this effect to the swelling of the microemulsion droplets after CO_2 is saturated with water. This phenomenon is parallel to what has been observed in other W/C microemulsion systems.[13] Because more water gets entrapped inside the droplets at larger W_0 values, the fraction of water dissolved in CO_2 continuous phase (f_A) becomes smaller and its contribution to D_{water} becomes less. Since D_{water/CO_2} is more than 10 times larger than D_{surf} (or D_{ME}), the observed decrease of D_{water} is expected when W_0 is increased.

Proton Spin Relaxation and Restricted Motion. Usually the dominant relaxation mechanism for protons is provided by the magnetic dipole−dipole interaction. The relaxation rates $R_1 = 1/T_1$ and $R_2 = 1/T_2$ resulting from dipole−dipole interactions depend on the correlation times for molecular reorientation and collisions and thus give indirect information about the sizes of molecules and aggregates. As a crude approximation to the relaxation rates, we consider only interactions in proton pairs in water and in the methylene groups on surfactant molecules. Also, we assume that the relevant correlation time τ_c results from rotational diffusion as described by the Debye−Einstein equation, $\tau_c = 4\pi a^3\eta/(3k_BT)$, where a is the molecular radius. The Bloembergen−Purcell−Pound theory (BPP) relaxation theory then provides estimates of R_1 and R_2.[22] In the extreme narrowing limit $\omega\tau_c \ll 1$, where ω is the Larmor frequency, it is well-known that $T_1 = T_2$.[23] This condition is met for small molecules in nonviscous solvents. For example, we dissolved Na−DiF_8 in methanol-d_4 and found T_1 and T_2 for the $-CH_2-$ groups to be 1.1 and 0.9 s, respectively. These values are equal within experimental error and confirm that Na−DiF_8 molecules do not undergo large-scale aggregation in methanol.

Parts A and B of Figure 3 show the T_1 and T_2 values, respectively, for water and surfactant ($-CH_2O-$) in the Na−DiF_8 W/C (water-in-CO_2) microemulsion system vs pressure with a surfactant concentration of 7 wt % and $W_0 \approx 9$. The T_1 and T_2 values for surfactant ($-CH_2-$) groups are considerably shorter than with methanol as solvent, and T_2 is less than T_1. These values indicate much longer rotation times for protons in $-CH_2-$, and the values are outside the extreme narrowing limit. This is consistent with the formation of microemulsion droplets.

The T_1 and T_2 values for water in microemulsion systems are significantly shorter than in bulk water and, in fact, are shorter than the values for the methylene protons. As in the diffusion measurements, the relaxation rate of water is the weighted average for water dissolved in the CO_2 continuous phase and the water inside the droplets. However, the water dissolved in the bulk CO_2 phase has relaxation times of the order of seconds and makes a very small contribution to the average relaxation rate. The observed relaxation rates indicate

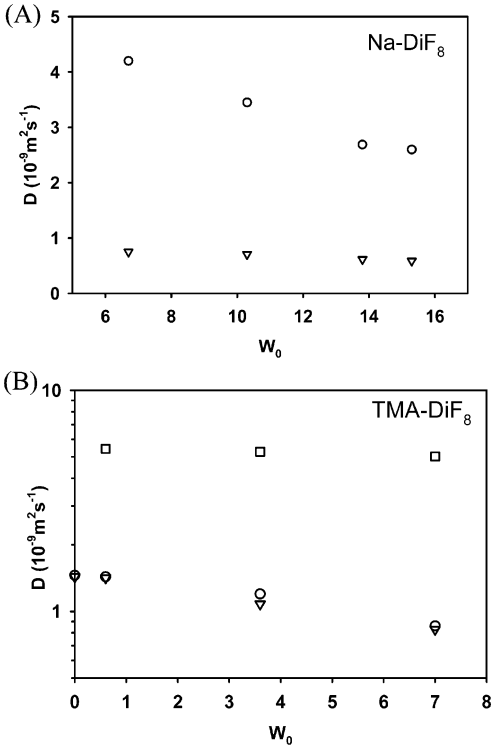

Figure 2. (A) Diffusion coefficients of components in W/C microemulsions formed with Na−DiF_8 at 25 °C, Na−DiF_8 2.5 wt %, around 204.1 bar: water (○) and surfactant tails (DiF_8,▽). (B) Diffusion coefficients of components in W/C microemulsions formed with TMA−DiF_8 at 25 °C, TMA−DiF_8 2.5 wt %, 204.1 bar: water (□), surfactant tails (DiF_8,▽), and counterions (TMA, ○).

that the water molecules in the microemulsion droplets have longer correlation times than the methylene groups in the surfactant tails. We conclude that the surfactant tails are relatively mobile while motion of water in the droplets is strongly restricted. When W_0 is small (<10), bulk water does not exist in the droplets where the entrapped water is mostly associated with headgroups.[24] The rotational correlation time for water is still considerably shorter than the rotational correlation time for a microemulsion droplet (with a radius between 2 and 3 nm) in CO_2. The BPP theory provides qualitative support for these ideas. Since the correlation times are not in the extreme narrowing limit, separate equations must be solved for T_1 and T_2, but no correlation time could be found that agrees quantatively with the measured T_2/T_1 ratio. To obtain better agreement with experiment, a more complete model with provision for intermolecular dipole−dipole interactions is required for the interior of the microemulsion droplets.

The relaxation rates for protons have also been measured for water, counterion (TMA), and surfactant ($-CH_2O-$) in the TMA−DiF_8 microemulsion systems at different W_0 values with a surfactant concentration of 2.5 wt % and a pressure of 204.1 bar. The results are shown in Figure 4A,B. For comparison, measurements were made for TMA−DiF_8 in methanol-d_4 solution. As with the Na−DiF_8 system, the reduced relaxation times in the W/C microemulsion system compared with the methanol solution and the inequality of T_1 and T_2 confirm the formation of large structures in CO_2; however, the dependence on W_0 is puzzling. There are competing factors at work. As W_0 increases, the droplets swell and their rotational correlation times increase. This effect alone would lead us to predict shorter spin relaxation times for protons. However, the increase in droplet radius produces larger internal volume and may lead to increased mobility for water molecules and something approaching free

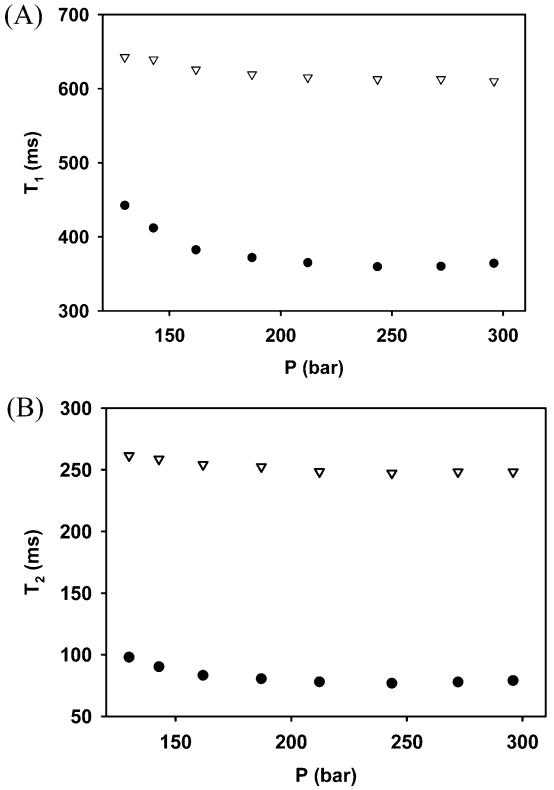

Figure 3. (A) Longitudinal relaxation time (T_1) of components in W/C microemulsions formed with Na−DiF_8 at 25 °C, Na−DiF_8 7 wt %, W_0 around 9: water (●) and surfactant tails (DiF_8,▽). (B) Transverse relaxation time (T_2) of components in W/C microemulsions formed with Na−DiF_8 at 25 °C, Na−DiF_8 7 wt %, W_0 around 9: water (●) and surfactant tails (DiF_8,▽).

or "bulk" water inside the droplets.[25] At the same time the increased radius of curvature is expected to increase the packing density of the surfactant tails and to decrease their mobilities. Figure 4 shows that these effects are quite small in the W_0 range from 0.5 to 7, except for the T_2 value of water protons which increase significantly in the range from 3.5 to 7. The increased water volume in the droplets does not have much effect on the mobility and relaxation time for the counterions. If the counterions mostly associate with headgroups, as predicted by the simulated pair distribution function,[26] the effect of the core size on their relaxation times will be small.

Proton Exchange in the A−DiF_8 Microemulsion System. From the 1D proton NMR spectra acquired at 25 °C for A−DiF_8 at 2.5 wt % and various W_0 values, it is found the resonances of H_2O and NH_4^+ are very broad. The apparent transverse relaxation time T_2 can be estimated with the equation $1/T_2 = \pi\Delta\nu_{1/2}$, where $\Delta\nu_{1/2}$ is the full width of the resonance at the half-height in hertz. The resulting T_2 values shown in Figure 5 are very small and are not consistent with reasonable rotational correlation times. Proton exchange between NH_4^+ and H_2O provides an explanation for the W_0 dependence of the T_2 values similar to that reported for the $PFPECOO^-NH_4^+$ microemulsion.[15]

To verify the existence of proton exchange, exchange spectroscopy (EXSY) measurements were performed with $W_0 \simeq 6$, a surfactant concentration of 2.5 wt %, and $d_8 = 0.1$ s. If exchange exists between two species, the intensities of corresponding cross-peaks should be positive in the EXSY spectrum. The spectra acquired at 25 and 4 °C (Figure 6) show resonances of NH_4^+ and H_2O at approximately 7 and 4 ppm. The positive cross-peaks confirm that exchange occurs even at 4 °C. We note there is some change in the position of the H_2O resonance when the temperature is changed.

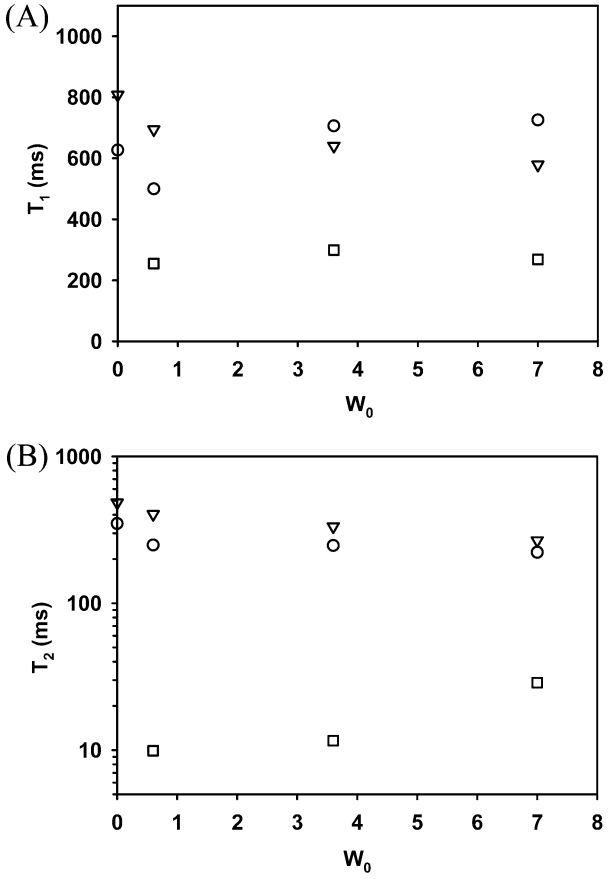

Figure 4. (A) Longitudinal relaxation time (T_1) of components in W/C microemulsions formed with TMA−DiF_8 at 25 °C, TMA−DiF_8 2.5 wt %, 204.1 bar: water (□), surfactant tails (DiF_8,▽), and counterions (TMA, ○). (B) Transverse relaxation time (T_2) of components in W/C microemulsions formed with TMA−DiF_8 at 25 °C, TMA−DiF_8 2.5 wt %, 204.1 bar: water (□), surfactant tails (DiF_8,▽), and counterions (TMA, ○).

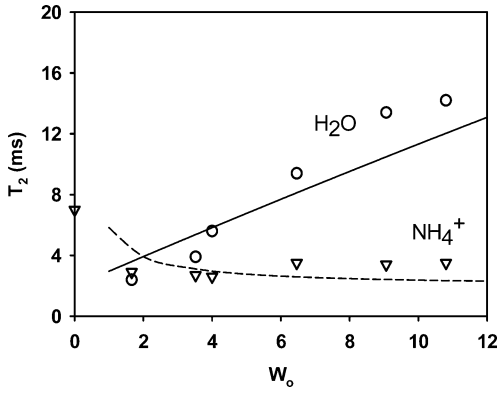

Figure 5. Transverse relaxation time (T_2) of NH_4^+ and H_2O in W/C microemulsions formed with A−DiF_8 at 25 °C, A−DiF_8 2.5 wt %, and 206.1 bar at various W_0.

In aqueous solutions of ammonium ions, a variety of mechanisms for exchange of protons between H_2O and NH_4^+ were studied by Grunwald et al.[27,28] The relevant exchange reactions for this work are shown in Scheme 3. The NMR spectra, T_2 measurements, and diffusion studies provide information about the rate constants. To begin with, the ammonium ion signal is always a singlet even though the J_{NH} coupling in NH_4^+ is approximately 53 Hz.[29] This is consistent with line narrowing by the rapid proton exchange between NH_4^+ and NH_3. Also, we note that the pH is only around 3,[30] which is

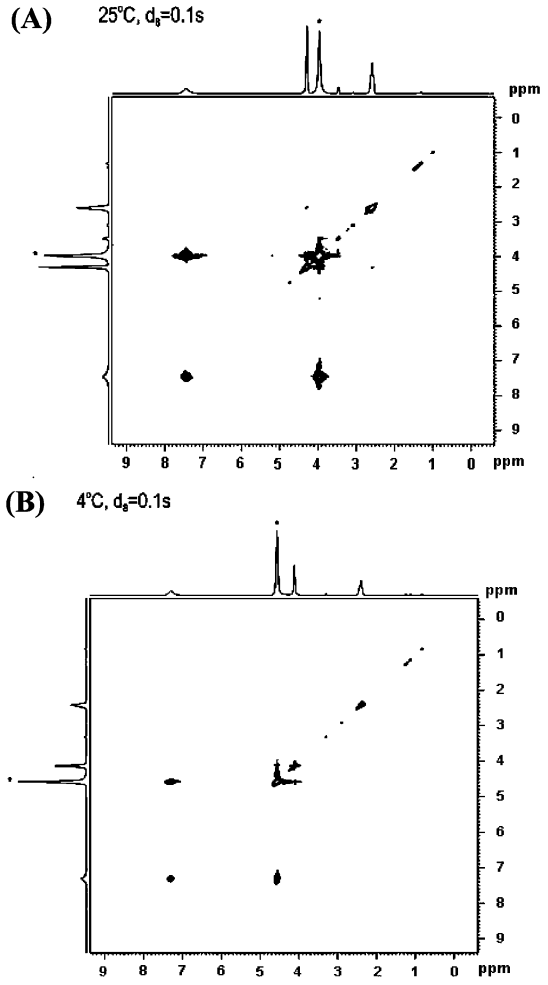

Figure 6. EXSY spectra for W/C microemulsions formed with A−DiF_8 when surfactant concentration of 2.5 wt %, W_0 around 6, and pressure of 206.1 bar. (A) was acquired at 25 °C; (B) was acquired at 4 °C.

SCHEME 3. Exchange Path in W/C Microemulsions Formed with A−DiF_8

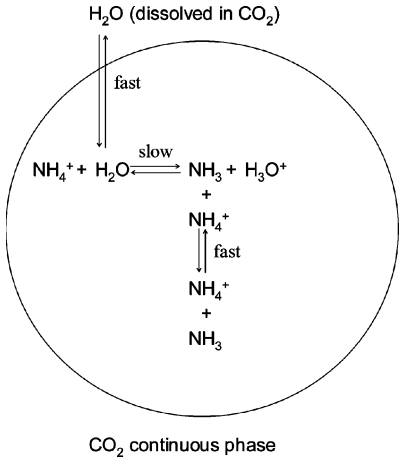

not acidic enough to slow down the exchange reaction and permit the resolution of the spin multiplet.[29]

The proton exchange between NH_4^+ and H_2O is slow compared with the chemical shift difference of these species and provides an explanation of W_0-dependent T_2 values that are shown in Figure 5. The simple two-site exchange model, where sites refer to locations having different chemical shifts, permits the mean lifetime of protons in the sites to be estimated from the measured T_2 values. A similar situation was found for the

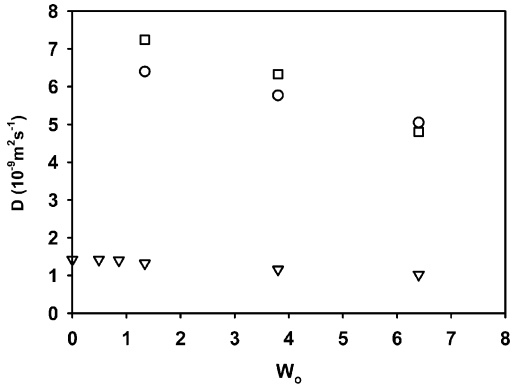

Figure 7. Diffusion coefficients for components in W/C microemulsions formed with A−DiF_8 at 25 °C and 206.1 bar with A−DiF_8 concentration of 2.5 wt % at various W_0: water (□), surfactant tails (DiF_8,▽), and counterions (NH_4^+, ○).

$PFPECOO^-NH_4^+$ microemulsion system.[15] The computed exchange rates are higher than those found in aqueous solutions of NH_4^+ and probably reflect the nonuniform distribution of ammonium ions and the nature of water binding to surfactant headgroups. Overall, the agreement of the exchange model, illustrated by the solid and dashed lines in Figure 5, with the experimental T_2 values confirms the basic validity of the proton exchange model.

NMR diffusion measurements analyzed with the assumption of single exponential decays for each component in A−DiF_8 microemulsion yielded the data shown in Figure 7. In strong contrast to observations on the TMA−DiF_8 microemulsion system, we found that the counterion (NH_4^+) has a large diffusion coefficient that is comparable to water and much larger than that of the surfactant tails. In the absence of water, it was found that the NH_4^+ signals have almost the same diffusion coefficient as the surfactant tails. The large diffusion coefficient associated with the NH_4^+ resonance is hard to understand. NH_4^+ is almost insoluble in CO_2, and if NH_3 escapes from the droplet, it would be expected to react with CO_2 to form a white precipitate of ammonium carbamate.

The proton exchange between NH_4^+ and H_2O again provides a plausible explanation. The rate appears to be slow because of the distinct resonances in the NMR spectrum. However, the time scale in the diffusion measurement is determined by the diffusion time Δ in the BPP−LED pulse sequence, and in our experiment the minimum diffusion time is $\Delta = 6.5$ ms. Exchanges occurring during this time interval will permit the proton to sample both the NH_4^+ and the H_2O sites. If the proton exchange time is much shorter than Δ, the measured diffusion coefficient will be the weighted average of the diffusion coefficients of NH_4^+ and H_2O. In the limit of slow exchange, the NH_4^+ and H_2O resonances will exhibit the diffusion coefficients of the separate species. Between these limits the situation is more complicated.

The effects of chemical exchange in PFG−NMR diffusion measurements have been discussed in detail.[31,32] In the case of two-site exchange model with different chemical shifts for the two sites, the signal intensity vs $q^2\Delta_r$ depends on four parameters: the diffusion coefficients of two species D_A (water) and D_B (NH_4^+); P_A, the fraction of spins in site A; and $k_A = 1/\tau_A$, the exchange rate for species in site A. Also, $P_B = 1 - P_A$, $k_A/k_B = (1 - P_A)/P_A$, and $k = k_A/P_B$. We can test this model by simulating the intensities of NH_4^+ and H_2O signals as functions of $q^2\Delta_r$ for various exchange rates.[32] At a particular W_0 value, P_A can be estimated with the assumption that the CO_2 continuous phase is saturated with water. The diffusion coefficient of water (D_A) is the weighted average of contribu-

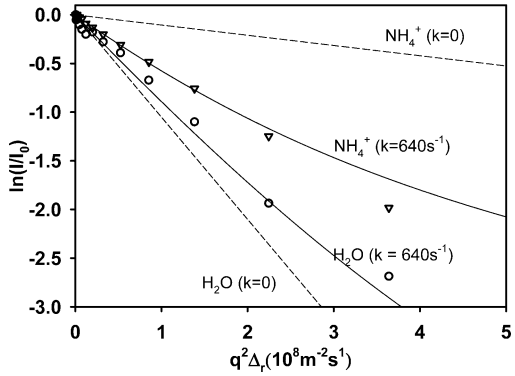

Figure 8. Simulation of two-site exchange model for signal decay in diffusion measurements of NH_4^+ and H_2O in W/C microemulsions formed with A−DiF_8 at 25 °C, A−DiF_8 2.5 wt %, and 206 bar when W_0 was around 4. k is the exchange rate. Dashed lines represent the simulation done at no exchange. Solid lines represent the simulation done at the exchange rate of 640 s^{-1}. Experimental data points are represented by open circles (for H_2O) and triangles (for NH_4^+).

tions from two sites: the water dissolved in CO_2 and the water entrapped in droplets. The diffusion coefficients for water dissolved in CO_2 at varied pressures and temperatures have been measured,[17] and the diffusion coefficients for water entrapped in droplets are assumed to equal to D_{surf}, the measured diffusion coefficients for droplets or surfactant tails. We also assume that the diffusion coefficient of NH_4^+ (D_B) is the equal to D_{ME}.

The equation used in this simulation are[32]

$$I_A(K,T) = \left[\frac{I_{A0}}{2} + \frac{(\mu I_{A0} + k_B I_{B0})}{2\Sigma}\right] e^{(-\sigma+\Sigma)T} + \left[\frac{I_{A0}}{2} - \frac{(\mu I_{A0} + k_B I_{B0})}{2\Sigma}\right] e^{(-\sigma-\Sigma)T} \quad (3)$$

$$I_B(K,T) = \left[\frac{I_{B0}}{2} - \frac{(\mu I_{B0} - k_A I_{A0})}{2\Sigma}\right] e^{(-\sigma+\Sigma)T} + \left[\frac{I_{B0}}{2} + \frac{(\mu I_{B0} - k_A I_{A0})}{2\Sigma}\right] e^{(-\sigma-\Sigma)T} \quad (4)$$

where I_A and I_B are the signal intensities of water and NH_4^+ at a diffusion time of T, $I_A = I_A(K,0)$, $I_B = I_B(K,0)$, and $K = \gamma g t$ is the area of the gradient pulse in cm^{-1} when t is the duration of the pulse gradient. Here T is the time between the second and third 90° pulses in a stimulated echo sequence and is slightly different from the diffusion time Δ. The functions σ, μ, and Σ in eqs 3 and 4 are defined as

$$\sigma = \frac{1}{2}[k_A + k_B + D_A K^2 + D_B K^2]$$

$$\mu = \frac{1}{2}[k_B - k_A + D_B K^2 - D_A K^2]$$

$$\Sigma = \sqrt{\mu^2 + k_A k_B}$$

Figure 8 shows the simulated results (solid lines) along with the measured signal intensities at 25 °C with $W_0 \approx 4.0$. The dashed lines represent intensities for H_2O and NH_4^+ in the absence of exchange ($k = 0$), and their slopes are D_A and D_B, respectively. It was found that an exchange rate of $k \simeq 640$ s^{-1} gives a satisfactory fit to the experimental points. This rate corresponds to the proton mean lifetime $\tau_B \simeq 1.6$ ms, which agrees with the measured T_2 value for NH_4^+ that is shown in Figure 5. This simple exchange model satisfactorily explains the anomalous diffusion coefficients measured for NH_4^+ in the A−DiF_8 microemulsion system.

We note that because of the exchange reaction the plots of $\ln(I/I_0)$ vs $q^2\Delta_r$ in Figure 8 are not linear. Therefore, the diffusion coefficients (Figure 7) obtained with the assumption of single-exponential decays, i.e., linear fits of logarithmic plots, are only apparent values. This effect leads to the erroneous conclusion that NH_4^+ diffuses much more rapidly than the surfactant tails.

SANS Analysis. The solutions were represented as a collection of polydisperse particles, assuming no orientational correlations, and the coherent differential scattering cross section is given by

$$\frac{dE}{d\Omega}(Q) = N_p[\langle |F(Q)|^2 \rangle + |\langle F(Q) \rangle|^2 (S(Q) - 1)] + B \quad (5)$$

where N_p is the number density of particles, $F(Q)$ is the particle form factor, $S(Q)$ is the structure function arising from interparticle scattering, and B is the background from CO_2 ($\sim$0.04 cm^{-1}, previously subtracted). Spherical particles with a centrosymmetric distribution of scattering length density may be modeled by concentric shells,[4] and for a core/shell micelle the intraparticle term in eq 5 may be expressed as

$$\langle |F(Q)|^2 \rangle = \int |F(Q,R_1)|^2 f(R_1)\, dR_1 \quad (6)$$

where R_1 is the radius of a core, which occurs within the distribution of core radii with a normalized frequency of $f(R_1)$. The form factor of a particle with core radius R_1 and outer radius R_2 is given by

$$F(Q,R) = \frac{4\pi}{3}[R_1^3(\rho_1 - \rho_2)F_0(Q,R_1) + R_2^3(\rho_2 - \rho_s)F_0(Q,R_2)]$$

$$F_0(x) = \frac{3}{x^3}(\sin x - x \cos x) \quad (7)$$

Several particle shapes have been used to calculate the intraparticle term (or form factor), and for in general for micelles in CO_2, the best fits have been given by a spherical core−shell model with a Schultz distribution[4] of particle sizes

$$f(R_1) = \frac{(Z+1)^{Z+1} X^Z \exp[-(Z+1)X]}{\overline{R_1}\,\Gamma(Z+1)}$$

$$Z = \frac{1 - \left(\frac{\sigma}{\overline{R_1}}\right)^2}{\left(\frac{\sigma}{\overline{R_1}}\right)^2}$$

$$X = \frac{R_1}{(\overline{R_2})^2} \quad (8)$$

where σ^2 is the variance of the distribution, Z is the breadth parameter, and ρ_1, ρ_2, and ρ_s are the scattering length densities (SLDs) of the core, shell, and solvent, respectively.

In the initial analysis of the data from phosphate fluorosurfactants in carbon dioxide,[3] particle interactions were neglected to a first approximation [$S(Q) \sim 1$] and $P(Q)$ was approximated[33] by $P(Q) \cong \exp[(-QR_g)^2/3]$. R_g is the radius of gyration, i.e., the rms distance of all scattering elements from the center of gravity, $R_g^2 = \Sigma f_k r_k^2 / \Sigma f_k$, and the summation runs over all scattering elements, k. Thus, typical (Guinier) plots of $\ln[I(Q)]$ vs Q^2 are linear, with slope, $R_g^2/3$, and the correspond-

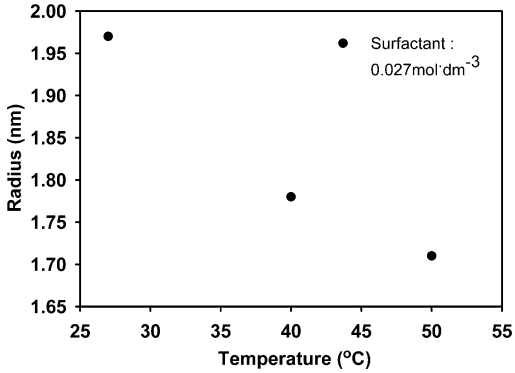

Figure 9. Temperature dependence of water droplet dimensions.

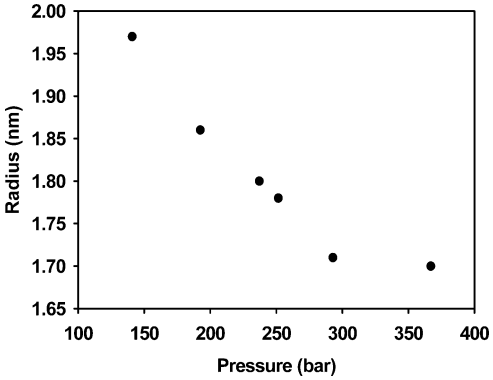

Figure 10. Pressure dependence of water droplet dimensions.

ing core radii are given by $R_1 = (5/3)^{0.5}R_g$. In a subsequent report,[4] we extended the initial analysis and allowed for polydispersity and also interparticle interactions between the droplets, which can cause $S(Q)$ to depart from unity. Following the formalism employed by Steytler,[34] Eastoe,[14] Lee,[12,13] and co-workers, $S(Q)$ was modeled via an attractive Ornstein−Zernike structure factor, characterized by a correlation length ξ and $S(0)$

$$S(Q) = 1 + \frac{S(0)}{1 + Q^2\xi^2} \tag{9}$$

Equation 9 has previously been applied[14,34] to account for interactions for surfactant concentrations ~0.05 mol dm^{-3}, and in this work the vast majority of samples were in a similar concentration regime (<0.03 mol dm^{-3}), with the exception of a few samples discussed below. SANS data were therefore analyzed initially assuming that the effect of particle−particle interactions was small, as previously observed[35] for values of W_0 in the range $4 < W_0 < 20$, where $S(Q)$ departed from unity only for high values ($W_0 > 30$) of the water/surfactant ratio. As the samples studied in this work were in the range $1.8 < W_0 < 7$, interparticle interactions would be expected to be small.

Allowance for particle polydispersity was made via eq 6 and allowing the Schultz breadth parameter to float generally resulted in values in the range $8 < Z < 16$. Similar polydispersity parameters have been observed[34,35] for other micelles formed by fluorosurfactants in CO_2. For a few systems with the highest values of W_0 (around 7) and D_2O content (up to 3.2 vol %), $S(0)$ was also allowed to "float", along with the correlation length, ξ. The latter generally gave values typically 70−100 Å, and the analysis was found to be insensitive to ξ in this range, as previously observed.[34,35] Fitting R_1, $S(0)$, and ξ, or fitting R_1, $S(0)$ with fixed $\xi \sim 100$ Å, generally gave values in the range $-0.1 < S(0) < 0.1$, confirming that the effect of interactions was small, even for the highest values of W_0 and the volume fraction (3.2%) of D_2O, as expected from previous studies of similar systems.[34,35] Thus, allowance for interactions generally changed R_1 by less than 3%, which is less than the overall uncertainty in R_1 (±2 Å) generally expected from SANS analysis for similar systems, and Table 1 shows the results after allowing for polydispersity and interactions. The W_0 values reported previously[3,4] and in the first column of Table 1 are based upon the amounts of surfactant and water added to the cell for each experiment.

As discussed previously,[3,4] the SLDs of the surfactant shell and CO_2 solvent are essentially matched ($\rho_2 \sim \rho_s$), so the scattering comes principally from the contrast between the D_2O core and CO_2. Thus, the water pools can be sized in terms of a core radius, R_1. Figure 9 shows that for a surfactant concentration of 0.027 mol dm^{-3} and an initial pressure of 140.9 bar, the core radius, R_1, falls 13% as the temperature is raised from 26 to 50 °C. An increase in temperature in this range affects the core radius even less (3−4% decrease) for surfactant concentration of 0.015 and 0.054 mol dm^{-3} (Table 1). Figure 10 shows that at the same temperature (27 °C) for fixed amounts of loaded water (W_0 around 5) and surfactant (0.027 mol dm^{-3}) R_1 falls around 14% as the pressure increases from 171.8 to 378.0 bar, consistent with the results of Eastoe and co-workers.[35] Core radii were also calculated via the Guinier analysis, used in the initial interpretation,[3] and despite the differences (~35%) in the absolute magnitudes of the radii derived from the two approaches, the same trends were observed in both analyses. However, the Guinier formalism assumes monodisperse particles, and we believe that the analysis described above better represents the structure of the actual micelles.

TABLE 1: Temperature and Pressure Dependence of Water Droplet Dimensions

W_0	surfactant (wt %)	surfactant (mol dm^{-3})	temp (°C)	press. (bar)	water droplet (core) radius (nm)
5.1	5.02	0.054	26	141.6	1.79
4.8	5.02	0.054	40	189.0	1.76
4.2	5.02	0.054	50	224.0	1.74
5.2	1.54	0.015	26	144.3	1.82
3.9	1.54	0.015	40	195.9	1.74
1.8	1.54	0.015	50	236.4	1.75
5.2	2.54	0.027	27	140.9	1.97
4.5	2.54	0.027	40	189.0	1.78
3.3	2.54	0.027	50	219.9	1.71
5.1	2.43	0.027	27	192.4	1.86
5.0	2.36	0.027	27	237.1	1.80
5.0	2.34	0.027	27	251.5	1.78
4.9	2.28	0.027	27	292.8	1.71
4.7	2.21	0.027	27	367.0	1.70
2.0	2.54	0.027	27	141.6	1.69
1.3	2.54	0.027	40	202.1	1.66
7.4	2.54	0.027	27	140.9	1.83
6.7	2.54	0.027	40	192.4	1.80
saturated	2.54	0.027	27	140.9	1.95
saturated	2.54	0.027	40	195.9	1.90

Configuration of A−DiF$_8$ Microemulsion System. SANS experiments were performed on the W/C microemulsion systems derived from Na−DiF$_8$ [3,4] and A−DiF$_8$ [16] in an effort to determine the geometries and sizes of the microemulsion droplets. Under conditions corresponding to 25 °C, 206.1 bar, $W_0 = 5$, and a surfactant concentration of 2.5 wt %, the diffusion coefficient for the surfactant tails (−CH_2CH_2O−) combined with the Stokes−Einstein equation yields a hydrodynamic radius of $R_h = 2.0$ nm. None of the SANS experiments summarized in Table 1 were performed at precisely this condition, but for similar conditions (surfactant 0.027 mol dm^{-3}, 27 °C, 192.4 bar, $W_0 = 5$), the radius of the microemulsion droplets is $R_1 =$

1.86 nm, and extrapolation to the *same* condition gives $R_1 = 1.87$ nm. This result implies $R_g = (3/5)^{0.5}R_1 = 1.45$ nm and $R_h = 1.87$ nm, assuming the theoretical ratio of $R_g/R_h = 0.775$ for a solid sphere.[36] We believe that the agreement is reasonable in view of the fact that the SANS and NMR techniques are weighted to measure somewhat different parts of the structure. Thus, as discussed above, the SLD contrast between the shell and the CO_2 medium is small, so the scattering comes principally from the contrast between the D_2O core and CO_2 and therefore monitors the size of the water pools in the *core* of the micelle.

Conclusions

NMR diffusion studies show that phosphorus fluorosurfactants (DiF_8 series with different counterions including Na^+, NH_4^+, and $N(CH_3)_4^+$) form W/C microemulsion droplets in liquid CO_2. The droplet radii are approximately 2 nm, and there is slight swelling as W_0 is increased in the range from about 1 to 10. Diffusion measurements show that the counterions diffuse with the droplets and have the same diffusion coefficients as the surfactant tails. In contrast to this behavior, water molecules exchange rapidly between the droplets and the bulk CO_2 phase, thus giving an average water diffusion coefficient much larger than that of the surfactant. The ^1H NMR relaxation and diffusion measurements for water and NH_4^+ in the $A-DiF_8$ system are determined by proton exchange reactions. The proton exchange rate is slow enough to permit distinct albeit broadened resonances for water and NH_4^+ but rapid enough for the proton to sample both water and NH_4^+ during the diffusion time. The result is that an apparent diffusion coefficient for the NH_4^+ signal is actually the average diffusion coefficient for an exchanging proton. Both the line widths and the diffusion coefficients for the $A-DiF_8$ system are adequately explained by a simple exchange model.

NMR relaxation measurements support the microemulsion model and give additional information about the state of water inside the droplets. The T_1 and T_2 values for water in the droplets are smaller than for methylene groups on the surfactant and T_1 is much larger that T_2. In the absence of exchange reactions, these values are determined primarily by rotational correlation times. The conclusion is that the motion of the water molecules is strongly restricted, and most water molecules are associated directly or indirectly with the surfactant headgroups. The rotational correlation time for water is clearly much less that that of the entire droplet but is longer than that for the relatively mobile surfactant tails.

SANS confirms the slight swelling of the micelles as W_0 is increased and has quantified the fall in the core radii (R_1) as the temperature is raised for different surfactant concentrations. In addition, for fixed W_0 and temperature, R_1 is inversely proportional to the pressure, and there is reasonable agreement between the micelle dimensions as measured by NMR and SANS.

Acknowledgment. This project was supported under NSF-STC Grant CHE-9876674 (J.M.D.) and NSF Grant CHE-9903723 (C.S.J.). We thank Dr. Jason Keiper and Tracy Bucholz for supplying samples. We also thank NIST for beam time for this project and Drs. Steve Kline and B. Hammouda for help with experiment arrangements at NIST. The research at Oak Ridge was sponsored by the Division of Materials Science and the Office of Biological and Environmental Research, supported by the U.S. Department of Energy under Contract DE-AC05-00OR22725 with the Oak Ridge National Laboratory, managed by UT-Battelle, LLC. We acknowledge the support of the National Institute of Standards and Technology, U.S. Department of Commerce, in providing the neutron research facilities used in this work.

References and Notes

(1) Fulton, J. L.; Pfund, D. M.; McClain, J. B.; Romack, T. J.; Maury, E. E.; Combes, J. R.; Samulski, E. T.; DeSimone, J. M.; Capel, M. *Langmuir* **1995**, *11*, 4241−4249.

(2) Johnston, K. P.; Harrison, K. L.; Clarke, M. J.; Howdle, S. M.; Heitz, M. P.; Bright, F. V.; Carlier, C.; Randolph, T. W. *Science* **1996**, *271*, 624−626.

(3) Keiper, J. S.; Simhan, R.; DeSimone, J. M.; Wignall, G. D.; Melnichenko, Y. B.; Frielinghaus, H. *J. Am. Chem. Soc.* **2002**, *124*, 1834−1835.

(4) Keiper, J. S.; Behles, J. A.; Bucholz, T. L.; Simhan, R.; DeSimone, J. M.; Lynn, G. W.; Wignall, G. D.; Melnichenko, Y. B.; Frielinghaus, H. *Langmuir* **2004**, *20*, 1065−1072.

(5) McFann, G. J.; Johnston, K. P.; Howdle, S. M. *AIChE J.* **1994**, *40*, 543−555.

(6) Consani, K. A.; Smith, R. D. *J. Supercrit. Fluids* **1990**, *3*, 51−65.

(7) Liu, Z. T.; Erkey, C. *Langmuir* **2001**, *17*, 274−277.

(8) Steytler, D. C.; Rumsey, E.; Thorpe, M.; Eastoe, J.; Paul, A. *Langmuir* **2001**, *17*, 7948−7950.

(9) Clarke, M. J.; Harrison, K. L.; Johnston, K. P.; Howdle, S. M. *J. Am. Chem. Soc.* **1997**, *119*, 6399−6406.

(10) daRocha, S. R.; Johnston, K. P. *Langmuir* **2000**, *16*, 3690−3695.

(11) Salaniwal, S.; Cui, S. T.; Cummings, P. T.; Cochran, H. D. *Langmuir* **1999**, *15*, 5188−5192.

(12) Lee, C. T., Jr.; Psathas, P. A.; Ziegler, K. J.; Johnston, K. P.; Dai, H. J.; Cochran, H. D.; Melnichenko, Y. B.; Wignall, G. D. *J. Phys. Chem. B* **2000**, *104*, 11094−11102.

(13) Lee, C. T.; Johnston, K. P.; Dai, H. J.; Cochran, H. D.; Melnichenko, Y. B.; Wignall, G. D. *J. Phys. Chem. B* **2001**, *105*, 3540−3548.

(14) Eastoe, J.; Bayazit, Z.; Martel, S.; Steytler, D. C.; Heenan, R. K. *Langmuir* **1996**, *12*, 1423−1424.

(15) Nagashima, K.; Lee, C. T., Jr.; Xu, B.; Johnston, K. P.; DeSimone, J. M.; Johnson, C. S., Jr. *J. Phys. Chem. B* **2003**, *107*, 1962−1968.

(16) Xu, B. PhD Disertation, University of North Carolina−Chapel Hill, 2004.

(17) Xu, B.; Nagashima, K.; DeSimone, J. M.; Johnson, C. S., Jr. *J. Phys. Chem. A* **2003**, *107*, 1−3.

(18) Wu, D.; Chen, A.; Johnson, C. S., Jr. *J. Magn. Reson. A* **1995**, *115* 260−264.

(19) Jerschow, A.; Müller, N. *J. Magn. Reson.* **1997**, *125*, 372−375.

(20) Wiebe, R. *Chem. Rev.* **1941**, *29*, 475−481.

(21) Senapati, S.; Berkowitz, M. L. *J. Chem. Phys.* **2003**, *118*, 1937−1944.

(22) Slichter, C. P. *Principles of Magnetic Resonance*, 3rd ed.; Springer-Verlag: New York, 1996.

(23) Farrar, T. C. *Introduction to Pulse NMR Spectroscopy;* Farragut Press: Chicago, 1989.

(24) Zulauf, M.; Eicke, H. F. *J. Phys. Chem.* **1979**, *83*, 480−486.

(25) Faeder, J.; Ladanyi, B. M. *J. Phys. Chem. B* **2000**, *104* 1033−1046.

(26) Senapati, S.; Keiper, J. S.; DeSimone, J. M.; Wignall, G. D.; Melnichenko, Y. B.; Frielinghaus, H.; Berkowitz, M. L. *Langmuir* **2002**, *18*, 7371−7376.

(27) Emerson, M. T.; Grunwald, E.; Kromhout, R. A. *J. Chem. Phys.* **1960**, *133*, 547−555.

(28) Grunwald, E.; Karabatsos, P. J.; Kromhout, R. A.; Purlee, E. L. *J. Chem. Phys.* **1960**, *33*, 556−563.

(29) Fraenkel, G.; Asahi, Y.; Batiz-Hernandez, H.; Bernheim, R. A. *J. Chem. Phys.* **1966,** *44*, 4647−4649.

(30) Niemeyer, E. D.; Bright, F. V. *J. Phys. Chem. B* **1998**, *102*, 1474−1478.

(31) Kärger, J.; Pfeifer, H.; Heink, W. *Advances in Magnetic Resonance;* Academic Press: New York, 1988; Vol. 12.

(32) Johnson, C. S., Jr. *J. Magn. Reson. A* **1993**, *102*, 214−218.

(33) Guinier, A.; Fournet, G. *Small-Angle Scattering of X-Rays*; Wiley: New York, 1955.

(34) Steytler, D. C.; Rumsey, E.; Thorpe, M.; Eastoe, J.; Paul, A.; Heenan, R. K. *Langmuir* **2001**, *17*, 7948.

(35) Eastoe, J.; Downer, A.; Paul, A.; Steytler, D. C.; Rumsey, E.; Penfold, J.; Heenan, R. K. *Phys. Chem. Chem. Phys.* **2000**, *2*, 5235.

(36) Wiltzius, P. *Phys. Rev. Lett.* **1987**, *58*, 710.